



HAL
open science

Sub-picosecond and nanometer scale dynamics of aluminum target surface heated by ultrashort laser pulse

F. Deneuville, B. Chimier, D. Descamps, F. Dorchies, S. Hulin, S. Petit, O. Peyrusse, J. J. Santos, C. Fourment

► To cite this version:

F. Deneuville, B. Chimier, D. Descamps, F. Dorchies, S. Hulin, et al.. Sub-picosecond and nanometer scale dynamics of aluminum target surface heated by ultrashort laser pulse. Applied Physics Letters, 2013, 102 (19), 10.1063/1.4807144 . hal-01561848

HAL Id: hal-01561848

<https://hal.science/hal-01561848>

Submitted on 27 May 2022

HAL is a multi-disciplinary open access archive for the deposit and dissemination of scientific research documents, whether they are published or not. The documents may come from teaching and research institutions in France or abroad, or from public or private research centers.

L'archive ouverte pluridisciplinaire **HAL**, est destinée au dépôt et à la diffusion de documents scientifiques de niveau recherche, publiés ou non, émanant des établissements d'enseignement et de recherche français ou étrangers, des laboratoires publics ou privés.

Sub-picosecond and nanometer scale dynamics of aluminum target surface heated by ultrashort laser pulse

Cite as: Appl. Phys. Lett. **102**, 194104 (2013); <https://doi.org/10.1063/1.4807144>

Submitted: 24 January 2013 • Accepted: 03 May 2013 • Published Online: 17 May 2013

F. Deneuille, B. Chimier, D. Descamps, et al.



View Online



Export Citation



CrossMark

ARTICLES YOU MAY BE INTERESTED IN

[The role of electron-phonon coupling in ultrafast laser heating](#)

Journal of Laser Applications **17**, 63 (2005); <https://doi.org/10.2351/1.1848522>

[Numerical simulation of ballistic electron dynamics and heat transport in metallic targets exposed to ultrashort laser pulse](#)

Journal of Applied Physics **124**, 065108 (2018); <https://doi.org/10.1063/1.5027401>

[Aurore: A platform for ultrafast sciences](#)

Review of Scientific Instruments **91**, 105104 (2020); <https://doi.org/10.1063/5.0012485>

Lock-in Amplifiers
up to 600 MHz



Zurich
Instruments



Sub-picosecond and nanometer scale dynamics of aluminum target surface heated by ultrashort laser pulse

F. Deneuille, B. Chimier, D. Descamps, F. Dorchies, S. Hulin, S. Petit, O. Peyrusse, J. J. Santos, and C. Fourment^{a)}

Université de Bordeaux-CNRS-CEA, Centre Lasers Intenses et Applications (CELIA), Talence F-33405, France

(Received 24 January 2013; accepted 3 May 2013; published online 17 May 2013)

The possibility of measuring surface hydrodynamics at picosecond and nanometer scales by using a time resolved optical interfero-polarimeter is demonstrated. This method is applied to observe the surface position of aluminum target heated by ultrashort laser pulse. Numerical simulations of the surface relaxation during a few tens of picoseconds after irradiation are in very good agreement with the measurements. Results show the important contribution of oxide layer in the surface dynamic evolution and the great accuracy of our experimental method. © 2013 AIP Publishing LLC. [<http://dx.doi.org/10.1063/1.4807144>]

Subpicosecond laser heating of solid matter is the field of active theoretical and experimental researches.^{1–13} In this regime, the laser energy is first absorbed by electrons and transferred to the lattice after the end of laser irradiation. The matter is out of equilibrium with different electron and ion temperatures during the electron-lattice coupling process (3–50 ps), and evolves from solid to warm dense matter (WDM). The study of this ultrafast dynamic associated with the system relaxation has brought a new set of fundamental questions regarding the time evolution of material properties.

Studying the surface motion of a metal sample during and after a subpicosecond laser irradiation presents a great interest to understand the material structural evolution along with the phase transition dynamics.^{14,15} An accurate description of the surface relaxation is essential to know the conditions of sample probed by an experimental tool or even by an *ab-initio* simulation. However, due to the fast transition to WDM state and relaxation, a picosecond or shorter time resolution is needed. In this time scale, the surface motion is in nanometer range, and the commonly used techniques (VISAR, shadowgraph, or radiography) are inadequate. Only optical interferometry of a probe laser beam reflecting on sample surface allows to reach these spatial and temporal resolutions.

Polarization resolved optical interferometry has proved its capability to deduce the local gradient length near the critical density of an expanding plasma with a subpicosecond time resolution, for gradient length larger than 10 nm.¹⁶ The plasma expansion is deduced from the comparison between the phase shifts of *S* and *P* components of a reflecting probe beam. Resonance absorption occurs only for *P*-polarized light, and phase shift difference between both polarization depends only on the gradient length around the critical density. However, for very steep gradients with a scale length lower than one hundredth of the probe wavelength, phase shifts are also sensitive to the modification of the material optical index in the over-critical region. The position of a

heated reflecting surface has also been inferred by optical interferometry,¹⁷ but the modification of the sample optical properties limited the accuracy to 10 nm. Until now, there was no possibility to separate the contribution of hydrodynamics from the variation of the material optical properties.

Here, we present a way to fulfill this challenge. It is based on polarization resolved measurement of both phase shift and reflectivity. It allows us to distinguish an *over dense expansion*—i.e., a global motion of the surface, with a null gradient length at the critical density (Fig. 1(a))—from a *plasma-type expansion* with a finite gradient length around the critical density (Fig. 1(b)). This technique is applied to measure the temporal surface evolution of an aluminum sample irradiated by a subpicosecond laser pulse. Our experimental results are compared to numerical simulations to explain the surface relaxation.

Let us first consider a sharp interface separating two homogeneous media of different optical indexes. We note $R_{s,p}^* = r_{s,p} e^{i\phi_{s,p}}$ the complex reflection coefficients for the *S* and *P* components of a probe beam reflecting on the surface. For an incidence angle of 45°, the Fresnel equations¹⁸ give $R_p^* = (R_s^*)^2$, and

$$r_p/r_s^2 = 1 \text{ and } 2\phi_s - \phi_p = 0. \quad (1)$$

We stress that relations 1 are independent of the refractive index of the material. They are thus still valid even if material optical properties are modified, for instance, by heating, as long as the interface remains steep. For this reason, if the sharp surface moves to a distance d (see Fig. 1(a)), $r_p/r_s^2 = 1$ is obviously still verified whatever the modification of the matter optical properties. However, a Doppler phase shift independent of the field polarization is then induced by the different propagation length of the light

$$\phi^{(D)} = \frac{4\pi \cos(\theta)d}{\lambda}, \quad (2)$$

where λ is the probe beam wavelength. In this case, $\phi_{s,p} = \phi_{s,p}^{(Fr)} + \phi^{(D)}$, where $\phi_{s,p}^{(Fr)}$ are the phase shift associated to the Fresnel equations—i.e., only to the matter optical

^{a)}Electronic mail: fourment@celia.u-bordeaux1.fr

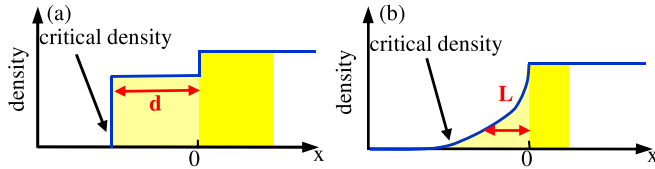


FIG. 1. Sketch of over-dense (a) and plasma-type (b) expansion.

properties. Since $2\phi_s^{(Fr)} - \phi_p^{(Fr)} = 0$, we get $2\phi_s - \phi_p = \phi^{(D)}$, which is proportional to the surface motion according to Eq. (2).

To explore the case of *plasma-type expansion* (Fig. 1(b)), numerical simulations are performed to estimate the reflexion of a probe beam in a transfer matrix formalism.¹⁹ We computed the reflexion of each polarization at 45° incidence on a plasma gradient of length L , where both electron density and collision frequency increase exponentially up to the values of the sample bulk. As soon as $L/\lambda < 10^{-4}$, the calculated complex reflectivities are very close to the ones given by the Fresnel equations ($r_p/r_s^2 = 1$ and $2\phi_s - \phi_p = 0$) and the surface can be considered as a sharp interface. For higher L , r_p/r_s^2 decreases while $2\phi_s - \phi_p$ becomes greater than zero. For $L/\lambda > 10^{-3}$, the ratio $r_p/r_s^2 < 0.97$ and $2\phi_s - \phi_p > 50$ mrad. These values are measurable by interferometry technique, so as one can deduce very small gradient length. Note that our simulations show that r_p/r_s^2 and $2\phi_s - \phi_p$ do not depend strongly on the electron density and collisionality in the bulk, but only on the plasma density gradient length.

Thanks to these properties, the surface dynamics of an aluminum sample irradiated by a femtosecond laser pulse was measured. Aluminum is a well documented material allowing accurate hydrodynamic simulations and is therefore a valuable test case for our diagnostic. An experiment was realized at CELIA (University of Bordeaux, France) using the Aurore Ti:sapphire laser (800 nm, 30 fs, up to 6 mJ at 1 kHz repetition rate). The laser beam was split into two beams. The pump beam was focused in S-polarization at 5° incidence angle within a $48 \mu\text{m}$ FWHM spot size on a 300 nm thick aluminum layer deposited on optical quality glass. Thanks to a rotating target holder, the sample was refreshed for kHz operation. The probe beam was used to set up a Frequency Domain Interferometry (FDI)²⁰ diagnostic. The probe beam was duplicated by passing through a Michelson interferometer, and a delay of 24 ps was set between each pulses. The beam was then focused at 45° incidence on the sample in a $\approx 200 \mu\text{m}$ focal spot. The reflected light of the probe beam was collected by an f/5 aperture aplanatic lens, which imaged the target surface on the entrance of a one meter focal length Fastie-Ebert imaging spectrometer. In the FDI absolute mode, the first probe pulse (the reference pulse) is reflected on the target before the pump interaction whereas the second one (the measuring pulse) is reflected after. Both probe pulses spectrally interfere in the spectrometer. A Fourier transform based algorithm is used to calculate the phase-shift and the reflectivity variation with respect to the unheated sample. In the relative mode,²⁰ the reference pulse is set to correspond to the measuring pulse of a previous measurement. This allows to probe the evolution at times larger than the two probe pulses delay of 24 ps. A

Wollaston cube was placed before the spectrometer CCD to make simultaneous measurements in both *S* and *P* polarizations. Accumulating 1000 shots for each delay and using a cooled 16-bits CCD allowed us to keep a low enough energy of the probe beam ($1 \mu\text{J}$ typical) to avoid nonlinear effects in the optics and to get high signal to noise ratio. This allowed us to measure reflectivity and phase shift with 1% and 10 mrad accuracy, respectively.

It is well known that nanometer oxide layer can be present at aluminum target surface. On our sample, a 7 – 10 nm layer of aluminum oxide was measured by ellipsometry technique. We stress that even at the maximum intensity of the pump beam in our experiment ($3 \times 10^{13} \text{ W} \cdot \text{cm}^{-2}$), the density of free electron in Al_2O_3 is 2–3 orders of magnitude lower than the critical density for the probe,²¹ leading to negligible absorption. As a consequence, the modification of the optical properties of the oxide layer by the pump beam is negligible.

Optical inspection of our sample after irradiation at different fluences showed that the damage threshold lay between 0.32 and $0.5 \text{ J} \cdot \text{cm}^{-2}$, and the ablation threshold was between 0.5 and $0.7 \text{ J} \cdot \text{cm}^{-2}$. The damage threshold fluence of metal layers deposited on dielectric substrates irradiated by a femtosecond laser depends on the film thickness and the heated depth.²² In our case, the film thickness is large enough for the target to be considered as a bulk sample. Indeed, the simulation presented below shows that significant heating (leading to the melting of the target) occurs only in the first 150 nm beyond the sample surface. Furthermore, a mechanical wave traveling at the sound speed in the sample cannot reach the sample surface after reflection at the film–substrate interface during the time of our study.

Figure 2 presents the temporal evolution of surface reflectivity (normalized to the ones of the cold sample) in *P* and *S* polarizations for aluminum target illuminated at $0.5 \text{ J} \cdot \text{cm}^{-2}$ and $1 \text{ J} \cdot \text{cm}^{-2}$, i.e., between the damage and ablation thresholds and above the ablation threshold, respectively. The reflectivities increase during the first picoseconds after the beginning of irradiation. At $0.5 \text{ J} \cdot \text{cm}^{-2}$ laser pump, they stay higher than the cold reflectivity, while they become lower for $1 \text{ J} \cdot \text{cm}^{-2}$ after 3 ps. This can be explained as follows: Absorption of 800 nm radiation in cold solid aluminum is dominated by interband transition.²³ Electrons and phonons heating leads to a decrease of this transition and an increase of the reflection.²⁴ Moreover, for these laser fluences, a solid-liquid phase transition occurs at the picosecond time scale.⁹ After this phase transition, the matter relaxation induces a decrease of reflectivity, which is more important for $1 \text{ J} \cdot \text{cm}^{-2}$ laser pump as the surface expansion may be greater than for $0.5 \text{ J} \cdot \text{cm}^{-2}$ laser pulse. Our measurements are in good qualitative agreement with those of Kandyla and co-workers in similar conditions.⁹ We notice however that Kandyla and co-workers attributed their results only to the temperature dependence during the solid-liquid phase transition and neglected the influence of a possible material density decrease induced by the surface relaxation, which also leads to an increase of the optical resistivity¹ and a decrease of the reflectivity. The technique we propose allows to get rid of such approximations.

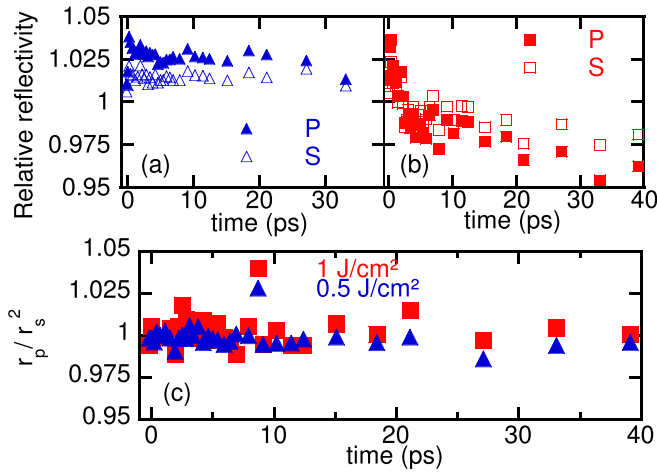


FIG. 2. Surface reflectivity evolution measured at 800 nm of Al sample irradiated by $0.5 \text{ J} \cdot \text{cm}^{-2}$ (a) and $1 \text{ J} \cdot \text{cm}^{-2}$ (b) laser pulses. The evolution of the ratio r_p/r_s is also presented (c).

The ratio r_p/r_s is plotted in Fig. 2(c). In both cases, it remains close to unity over the 40 ps of the scan, in spite of the evolution of the optical properties of the material described here above. This shows unambiguously that the sample undergoes an *over dense expansion* where the Fresnel relations are relevant (Eq. (1)). Calculating $2\phi_s - \phi_p$ from the measured phase shifts, the surface motion can be deduced directly by using Eq. (2). The results are shown in Fig. 3 (experimental points) where three different steps can be identified in the measured aluminum surface motion. During the first 5 ps, the Al-oxide interface moves toward vacuum with a velocity of 0.6 nm/ps and 1 nm/ps for $0.5 \text{ J} \cdot \text{cm}^{-2}$ and $1 \text{ J} \cdot \text{cm}^{-2}$, respectively. After, one can observe a slowing down of the surface expansion during 10 ps for $0.5 \text{ J} \cdot \text{cm}^{-2}$, and 5 ps for $1 \text{ J} \cdot \text{cm}^{-2}$. Next, the surface moves with a constant velocity, which depends on the pump fluence (0.1 nm/ps for $0.5 \text{ J} \cdot \text{cm}^{-2}$, and 0.4 nm/ps for $1 \text{ J} \cdot \text{cm}^{-2}$). Interestingly, the surface velocity tends to vanish at $0.5 \text{ J} \cdot \text{cm}^{-2}$, in agreement with the fact that no aluminum ejection was detected on post-irradiation inspection. The initial values of the surface velocities are in qualitative agreement with the velocities of heavy nanoparticles measured in similar conditions,⁷ but performed on a laser cleaned sample (where the oxide layer was likely to be removed) and with a 5 ns time resolution. This suggests that the expanding liquid

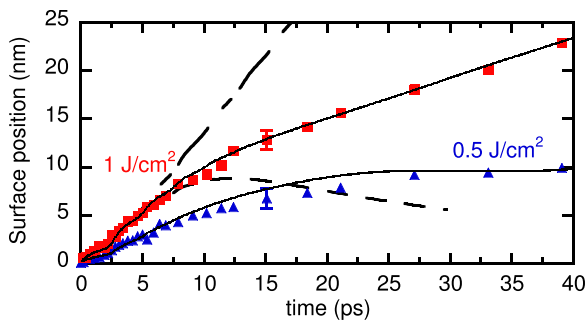


FIG. 3. Measured and calculated Al surface position of an aluminum sample overcoated by a 10 nm oxide layer, irradiated by $0.5 \text{ J} \cdot \text{cm}^{-2}$ (blue triangles and corresponding line) and $1 \text{ J} \cdot \text{cm}^{-2}$ (red squares and corresponding line) laser pulses. The results obtained without mechanical resistance (dotted-dashed line), and with constant stretching force (dashed line), are also presented for the $1 \text{ J} \cdot \text{cm}^{-2}$ case.

layer at the surface may decompose into nanoparticles, but in our experiment, this decomposition did not occur during the first 40 ps in the few tens of nanometers beyond the surface probed by our diagnostic.

Simulations were performed with 1D Lagrangian hydrodynamic code ESTHER.²⁵ The Helmholtz wave equation is solved to determine the electromagnetic field through the region illuminated by the laser, and the deposited energy is deduced using the Joule-Lenz law. In the calculation, the sample was composed of a 300 nm aluminum target overcoated by a 10 nm thick oxide film. The oxide layer is transparent at 800 nm light with a constant optical index of 1.76. The pump laser energy is absorbed by the aluminum electrons behind the Al-oxide interface. The deposited laser energy is transferred to the aluminum lattice after the end of pump irradiation. A two-temperature equation of state²⁵ based on the multiphase equilibrium equation of state Bushman, Lomonosov and Fortov²⁶ is used for aluminum, and aluminum oxide is described by the SESAME table 7411. To include the oxide mechanical resistance in our 1D simulation, the oxide layer is assimilated to a membrane—i.e., a thin plate subject to large external stretching forces applied at its circumference. By assuming the extension of this membrane similar in all directions, the mechanical resistance pressure can be written as²⁷ $P_r = T_r \Delta_r \zeta$, where r is the radial coordinate, T_r the absolute magnitude of the stretching force, and ζ the surface position. By taking $\zeta = d(R^2 - r^2)/R^2$ in cylindrical coordinates, with d the calculated surface position in ESTHER and $R = 40 \mu\text{m}$ the membrane radius, $P_r = -4d T_r / R^2$.

First, the simulation show *over dense expansions* for $1 \text{ J} \cdot \text{cm}^{-2}$ laser fluence only when the oxide layer is present. In this case, the aluminum boundary stays sharp due to the oxide mass in front of it. The calculated Al–Al₂O₃ interface motion are presented in Fig. 3. When an oxide layer without mechanical resistance is considered (dotted-dashed line), the calculated surface position coincides with the experimental measures only during the first five picoseconds but at higher delays, the surface velocity keeps a high value. With a constant stretching force (dashed line), the mechanical resistance is too high after 10 ps, leading to a surface contraction. We conclude that the stretching force decreases as the time increases since the oxide layer breaks slowly under the effect of aluminum expansion. To include this effect, $T_r = T_0 \exp(-t/t_i)$ in the resistance pressure expression (full line). In our simulation $T_0 = 4 \text{ GPa} \cdot \mu\text{m}$, and the characteristic breaking time t_i depends on the laser fluence: $t_i = 18 \text{ ps}$ for $0.5 \text{ J} \cdot \text{cm}^{-2}$ and 13 ps for $1 \text{ J} \cdot \text{cm}^{-2}$. Finally, we stress that no spall layer is observed in the few tens of nanometer probed beyond the surface. Such a layer has been predicted by hydrodynamic simulations,¹⁴ due to a negative pressure zone accompanying a free surface relaxation. Our simulations showed however that this negative pressure is inhibited by the presence of the oxide, which is denser than aluminum.

In summary, measuring both reflectivity and phase shift in *S* and *P* polarisations allows to discriminate between under dense and over dense expansion. Up to the maximum fluence of our experiment ($1 \text{ J} \cdot \text{cm}^{-2}$), neither under dense expansion nor liquid-vapor dissociation occurs in the probed thickness of the sample, during the first 40 ps after heating.

Simulations show that this is partly due to the ≈ 10 nm oxide layer at the Al sample surface. In addition, the position evolution of the aluminum surface is measured with an unprecedented 1 nm accuracy, 5 μm lateral resolution, and sub-100 fs temporal resolution. We showed that the oxide layer restrains the aluminum expansion and slows down the surface motion during the first ten picoseconds after laser irradiation. We believe that the experimental method presented in this paper is a fantastic tool to study surface dynamic features during phase transitions, including nanobumps formation or spallation,²⁸ electron sheath, and coulombic explosion.² Furthermore, the technique presented in this work should be useful to correct for eventual hydrodynamic contribution to reflectivity or phase shift measurement of heated matter aiming at the determination of dielectric function.

We acknowledge R. Bouillaud, F. Burgy, A. Le Goff, C. Medina, and L. Merzeau for their technical assistance. We thank J. P. Geindre and P. Audebert for valuable discussions and help in setting up and using FDI. We thank P. Combis and L. Videau for giving access to the ESTHER code. This work was supported by the French Agence Nationale de la Recherche, under grant OEDYP (ANR-09-BLAN-0206-01) and the Conseil Régional d'Aquitaine, under grants POLUX (2010-13-04-002) and COLA2 (2.1.3 09010502).

- ¹K. Eidmann, J. Meyer-ter-Vehn, T. Schlegel, and S. Huller, *Phys. Rev. E* **62**, 1202 (2000).
²R. Stoian, A. Rosenfeld, D. Ashkenasi, I. V. Hertel, N. M. Bulgakova, and E. E. B. Campbell, *Phys. Rev. Lett.* **88**, 097603 (2002).
³D. Perez and L. J. Lewis, *Phys. Rev. Lett.* **89**, 255504 (2002).
⁴B. J. Siwick, J. R. Dwyer, R. E. Jordan, and R. J. D. Miller, *Science* **302**, 1382 (2003).
⁵S. Eliezer, N. Eliaz, E. Grossman, D. Fisher, I. Gouzman, Z. Henis, S. Pecker, Y. Horovitz, M. Fraenkel, S. Maman, and Y. Lereah, *Phys. Rev. B* **69**, 144119 (2004).

- ⁶T. E. Glover, G. D. Ackerman, R. W. Lee, H. A. Padmore, and D. A. Young, *Chem. Phys.* **299**, 171–181 (2004).
⁷S. Amoroso, R. Bruzzese, M. Vitiello, N. N. Nedialkov, and P. A. Atanasov, *J. Appl. Phys.* **98**, 044907 (2005).
⁸T. Ao, Y. Ping, K. Widmann, D. F. Price, E. Lee, H. Tam, P. T. Springer, and A. Ng, *Phys. Rev. Lett.* **96**, 055001 (2006).
⁹M. Kandyla, T. Shih, and E. Mazur, *Phys. Rev. B* **75**, 214107 (2007).
¹⁰K. Oguri, Y. Okano, T. Nishikawa, and H. Nakano, *Phys. Rev. Lett.* **99**, 165003 (2007).
¹¹R. Ernstorfer, M. Harb, C. T. Hebeisen, G. Sciaini, T. Dartigalongue, and R. J. D. Miller, *Science* **323**, 1033 (2009).
¹²F. Dorchies, A. Levy, C. Goyon, P. Combis, D. Descamps, C. Fourment, M. Harmand, S. Hulin, P. M. Leguay, S. Petit, O. Peyrusse, and J. J. Santos, *Phys. Rev. Lett.* **107**, 245006 (2011).
¹³K. H. Bennemann, *J. Phys.: Condens. Matter* **23**, 073202 (2011).
¹⁴M. E. Povarnitsyn, T. E. Itina, K. V. Khishchenko, and P. R. Levashov, *Phys. Rev. Lett.* **103**, 195002 (2009).
¹⁵D. S. Ivanov and L. V. Zhigilei, *Phys. Rev. Lett.* **91**, 105701 (2003).
¹⁶P. Blanc, P. Audebert, F. Fallies, J. P. Geindre, J. C. Gauthier, A. D. Santos, A. Mysyrowicz, and A. Antonetti, *J. Opt. Soc. Am. B* **13**, 118 (1996).
¹⁷V. V. Temnov, K. Sokolowski-Tinten, P. Zhou, and D. von der Linde, *J. Opt. Soc. Am. B* **23**, 1954 (2006).
¹⁸M. Born and E. Wolf, *Principles of Optics*, 7th ed. (Cambridge University Press, 1999), p. 42.
¹⁹L. A. A. Pettersson, L. S. Roman, and O. Ingans, *J. Appl. Phys.* **86**, 487 (1999).
²⁰J. P. Geindre, P. Audebert, A. Rousse, F. Fallières, J. C. Gauthier, A. Mysyrowicz, A. D. Santos, G. Hamoniaux, and A. Antonetti, *Opt. Lett.* **19**, 1997 (1994).
²¹F. Quéré, S. Guizard, and Ph. Martin, *Europhys. Lett.* **56**, 138 (2001).
²²S.-S. Wellershoff, J. Hohlfeld, J. Gdke, and E. Matthias, *Appl. Phys. A* **69**, S99 (1999).
²³N. W. Ashcroft and K. Sturm, *Phys. Rev. B* **3**, 1898 (1971).
²⁴D. Fisher, M. Fraenkel, Z. Henis, E. Moshe, and S. Eliezer, *Phys. Rev. E* **65**, 016409 (2001).
²⁵J. P. Colombier, P. Combis, F. Bonneau, R. Le Harzic, and E. Audouard, *Phys. Rev. B* **71**, 165406 (2005).
²⁶A. V. Bushman, I. V. Lomonosov, and V. E. Fortov, *Sov. Technol. Rev. B* **5**, 1 (1993).
²⁷L. D. Landau and E. M. Lifshitz, *Theory of Elasticity, A Course of Theoretical Physics* (Pergamon Press, 1970), Vol. 7.
²⁸T. V. Kononenko, S. M. Pimenov, V. V. Kononenko, E. V. Zavedeev, V. I. Konov, G. Dumitru, and V. Romano, *Appl. Phys. A* **79**, 543 (2004).